Separation Science and Technology
Publication details, including instructions for authors and subscription information:
http://www.informaworld.com/smpp/title~content=t713708471

AQUA-IMPREGNATED RESINS AS NEW DUAL-FUNCTION DEUTERATING AGENT

Dmitri Muraviev[ab]; Abraham Warshawsky[b]
[a] Department of Analytical Chemistry, Autonomous University of Barcelona, Barcelona, Spain [b] Department of Organic Chemistry, The Weizmann Institute of Science, Rehovot, Israel

To cite this Article Muraviev, Dmitri and Warshawsky, Abraham(2001) 'AQUA-IMPREGNATED RESINS AS NEW DUAL-FUNCTION DEUTERATING AGENT', Separation Science and Technology, 36: 8, 2087 — 2119
To link to this Article: DOI: 10.1081/SS-100104767
URL: http://dx.doi.org/10.1081/SS-100104767

SEPARATION SCIENCE AND TECHNOLOGY, 36(8&9), 2087–2119 (2001)

AQUA-IMPREGNATED RESINS AS NEW DUAL-FUNCTION DEUTERATING AGENT

Dmitri Muraviev* and Abraham Warshawsky

Department of Organic Chemistry,
The Weizmann Institute of Science, Rehovot 76100, Israel

ABSTRACT

This study reviews our work on novel approaches for carrying out hydrogen-deuterium (H-D) exchange reactions, culminating in a process to produce extremely pure deuterated organic compounds using solid (polymeric) reagents, e.g., cation exchangers in the deuterium form pre-swollen in deuterium oxide (D_2O). H-D exchange reaction carried out by cation-exchange deuterating agents in a tri-phase liquid-liquid-solid systems (TMAB solution in CCl_4-D_2O-resin in the D-form) is accompanied by significant hydrolysis of both TMAB and TMAB-d_3 (deuterated TMAB). Substitution of the liquid aqueous phase by D_2O taken up by the swollen resin phase eliminates the hydrolytic side-reaction. Hydrogen-deuterium exchange reaction on TMAB catalyzed by cation-exchange resins or membranes under batch or under dynamic conditions, in columns, results in 100% yield of spectroscopically pure TMAB-d_3.

---

*Corresponding author. Current address: Department of Analytical Chemistry, Autonomous University of Barcelona, E-08193 Bellaterra, Barcelona, Spain. Fax: 34-93-5812379; E-mail: Dimitri.Muraviev@uab.es

INTRODUCTION

Current practical methods for labeling compounds fall into three main categories (1–3): 1) chemical synthesis; 2) isotope-exchange reactions; and 3) biochemical methods. The first two general methods are of particular importance when applied for labeling compounds with deuterium (and tritium). Synthesis of organic compounds stereospecifically labeled with hydrogen isotopes has proven to be the most powerful tool allowing for elucidation of chemical and biochemical reaction mechanisms (3,4), and for structural characterization of organic compounds (5).

Many types of organic compounds may be readily labeled with the hydrogen isotopes under appropriate conditions for different isotope-exchange reaction. A good understanding of factors responsible for isotope-exchange reactions will improve the yields of the labeled products Labeling of the substrate compound must be carried out under optimal conditions i.e., 1) exchange reactions are both rapid and efficient and 2) side-reactions are minimized.

Commercially available alkali metal borodeuterides are effectively employed for selective introduction of deuterium into organic compounds containing reducible functional groups (1,6). Deuterated trialkylamine boranes and trimethylamine borane (TMAB) in particular, are the most important intermediates for their synthesis. Synthetic procedure involves one stage where TMBA-d_3 (deuterated TMAB) reacts with, e.g., sodium methoxide evolving trimethylamine and sodium borodeuteride (7,8).

Our interest in monoisotopic forms of sodium borohydride (e.g., tritium-free $NaBH_4$) has arisen because of our involvement with the solar neutrino experiments at Grna-Sasso (Italy) known as the Gallex experiment. The Weizmann Institute of Science was one of the partners in this experiment (9). In this project, sodium borohydride is applied to reduce $GeCl_4$ into GeH_4 in gallium detector based on the neutrino capture reaction (10,11):

$$^{71}\mathrm{Ga} \xrightarrow{(\nu e,\bar{e})} {}^{71}\mathrm{Ge}$$

Deuterated alkali metal borohydrides are also suggested to be appropriate candidates for this purpose.

Trialkylamine boranes have been known since 1937 (12–14) and are widely used as selective reducing and hydroborating agents in organic synthesis (15–18) and for metal reduction (19–21). The hydrogen-deuterium exchange of boron-bound hydrogens in TMAB was originated by Davis et al. (22) and later reinvestigated (in a scaled-up process) by Atkinson et al. (7,8). The isotope-exchange reaction on TMAB is carried out in the liquid-liquid extraction system by consequential treatment of an etheric TMAB solution by consecutive portions of D_2SO_4 (10 times) and is based on the exchange interaction of boron hydrogens with deuterons (23):

$$(CH_3)_3NBH_3 + 1.5\ D_2SO_4 \Leftrightarrow (CH_3)_3NBD_3 + 1.5\ H_2SO_4 \qquad (1)$$

Marcel Dekker, Inc.
270 Madison Avenue, New York, New York 10016

Hydrogen-deuterium (H-D) exchange reaction (1) on TMAB (and other trialkylamine boranes) is known to be coupled with rather intensive hydrolysis (7,8,22) leading to the release of hydrogen (H_2 or HD), boric acid, and trimethylamine (24–26):

$$\begin{aligned}&(CH_3)_3NBH_3 + H^+(D^+) + 3H_2O(D_2O)\\&\qquad\Rightarrow (CH_3)_3H^+ + B(OH)_3(B(OD)_3) + 3H_2(HD)\end{aligned} \tag{2}$$

The hydrolysis results in a decreased yield of the final TMAB-d_3 product (around 60% according to the standard procedure described (1). Hence, H-D exchange on TMAB can be considered as a typical example of isotope-exchange reaction accompanied by undesired side-interaction.

Hydrolysis of TMAB (and deuterolysis of TMAM-d_3) is of particular interest. In synthetic applications, the excess reducing agent can be removed by hydrolytic destruction (e.g., with aqueous acid (17)). In the acid-catalyzed hydrogen-deuterium exchange on TMAB, the hydrolysis is an undesired reaction. A detailed investigation of the kinetics of TMAB hydrolysis with mineral acids has been carried out by Ryschkevitch (24) and Davis et al. (23). For obvious reasons, the hydrolysis of TMAB has been assumed to be an acid-catalyzed reaction (23,24), but until recently, no evidences for this can be found in the literature. Moreover, quite curiously, the hydrolysis of TMAB was shown to be an auto-catalytic process accelerated by the hydrolytic product, namely trimethylammonium ions (24) (see reaction (2)). The following main reasons have stimulated the authors to start the series of investigations described in this study:

1. None of the publications describing deuteration of TMAB have reported (until recently) any quantitative data on the rates of the isotope-exchange reaction or those on the accompanying hydrolysis reaction, although information of this type is available in some publications concerning deuteration of boranes (27–32),
2. The use of solid (polymeric) deuterating agents has not been described in the literature, and
3. An overall kinetic mechanism of H-D exchange reaction on TMAB has not been reported until recently.

The study summarizes the results obtained by developing the novel approach for carrying out the hydrogen-deuterium exchange reactions. The approach is based on the use of solid polymeric deuterating agents such as, sulfonate cation exchangers in the D-form pre-swollen in D_2O. Hydrolysis of TMAB in the presence of liquid and solid (polymeric) acids, hydrogen-deuterium exchange reaction on TMAB with cation-exchange resins or membranes under batch or dynamic conditions (in column), and results obtained by studying some other problems are reported and discussed below.

GENERAL BACKGROUND

The following materials were used in the studies described below: TMAB was synthesized and purified as described elsewhere (33). Standard deuterated TMAB-d_3 was prepared by reacting sodium borodeuteride with trimethylamine hydrochloride (34). Samples of granulated sulfonate cation exchanger Dowex 50 × 2 (40–60 mesh) were transformed into the deutero-form (D-form) according to the procedure described earlier (35). The cation-exchange membranes composed of highly sulfonated polyethylene were supplied by Soreq Nuclear Research Center, Israel. Carbon tetrachloride was used as a solvent for TMAB in all experiments carried out due to a combination of required water insolubility and favorable spectroscopic properties. The isotope-exchange reaction was monitored by Fourier transform infrared (FTIR) analysis following the disappearance of the strong B-H absorption band at 2360 cm^{-1} and the appearance of the broad B-D band at 1783 cm^{-1}, indicating BH_3 and BD_3 antisymmetric stretches, respectively (36). The kinetics of TMAB hydrolysis was studied under batch conditions as described elsewhere (37,38) and was followed by both FTIR analysis and volumetric measurements of the gas evolving the reactor (see Eq. 2). From the results of FTIR analysis the degree of hydrolysis (F_H) was calculated as follows:

$$F_H = \frac{C_o - C_t}{C_o} \tag{3}$$

where C_t and C_o are the concentration of TMAB at time t and at $t = 0$ (initial), mol/dm^3.

From the results of the volumetric analysis, the F_H values were calculated independently for the same time intervals according to

$$F_H = \frac{V_t}{V_{\max}} \tag{4}$$

where V_t is the volume of hydrogen (or HD) evolved in the time interval, t, and V_{max} is the maximum volume of the gas that evolves from a given amount of TMAB under complete hydrolysis at normal conditions (273.15 K and 1 bar) according to Eq. (2).

D-H EXCHANGE REACTION ON TMAB WITH SULFONATE CATION EXCHANGER IN DEUTERIUM FORM UNDER BATCH CONDITIONS

The main parameters of the systems (S_1 to S_6) described in this section are collected in Table 1. S_1 is similar to the liquid-liquid biphase systems studied by Davis et al. (22) or Atkinson et al. (7,8). Systems S_2 and S_3 are triphase systems

Table 1. Parameters of Systems Used by Studying H-D Exchange on TMAB with Ion-Exchange Resins*

System No.	Number of Phases	Aqueous Phase	Type of System	Solid Phase	Reaction Studied	Remarks
S_1	2	1.6 M D_2SO_4 in D_2O	O/A	—	H-D exchange	Hydrolysis of TMAB was observed but not measured quantitatively
S_2	3	D_2O pD ≈ 6	O/A/R	Dowex 50 × 2	H-D exchange and hydrolysis	Resin granulation 40–60 mesh
S_3	3	D_2O pD ≈ 6	O/A/R	Dowex 50 × 8	H-D exchange	Resin granulation 200–400 mesh
S_4	2	—	O/-/R	Dowex 50 × 2	H-D exchange and hydrolysis	Resin granulation 40–60 mesh; resin phase was preliminarily swollen in D_2O and washed from the sorbed D_2SO_4
S_5	2	—	O/-/R	Dowex 50 × 2	H-D exchange and hydrolysis	Resin granulation 40–60 mesh; sorbed D_2SO_4 was not removed from resin phase
S_6	3	0.14 M TMA in D_2SO_4 pD ≈ 6	O/A/R	Dowex 50 × 2	H-D exchange and hydrolysis	Resin granulation 40–60 mesh

* pD = $-\log[D^+]$; TMA = trimethylamine; O = organic phase (15 mL of 0.1 M TMAB in CCl_4); A = aqueous phase (15 mL); R = resin phase (2.5 mEq of SO_3^- groups); — = none. Reprinted with permission from Muraviev et al. (35). Copyright [1994] American Chemical Society.

in which the resin phase (Dowex 50 with 2% divinylbenzene (DVB) in S_2 and 8 % DVB in S_3), carrying 20 times less amounts (than in S_1) of sulfonic acid groups, was employed. The difference between S_2 and S_3 (besides cross-linkage) is also in resin granulation (40–60 mesh in S_2 versus 200–400 mesh in S_3). In systems S_4

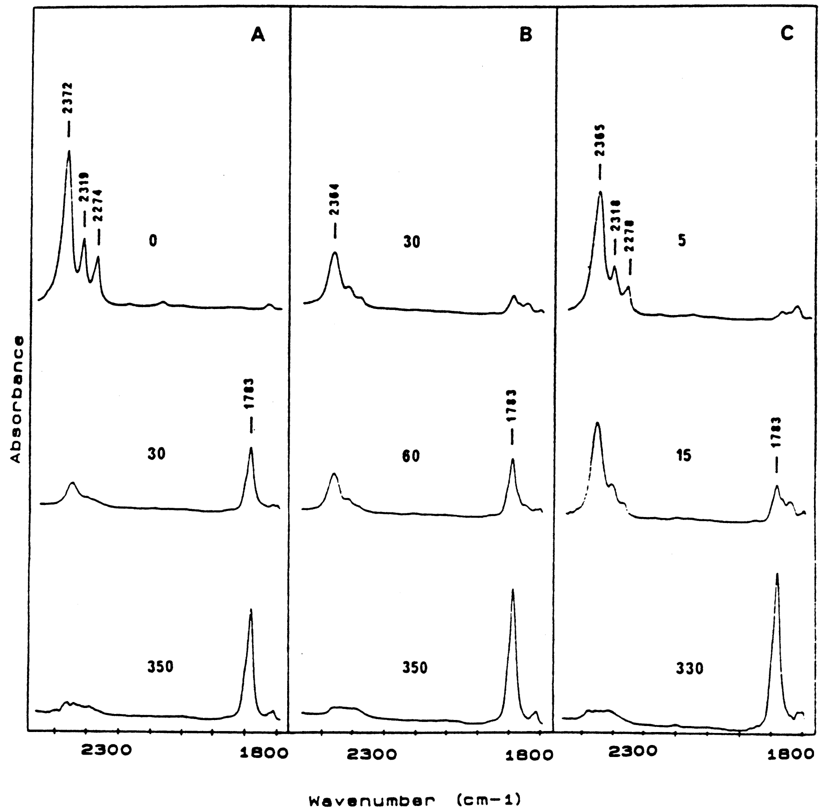

Figure 1. Typical FTIR spectra of organic phase containing TMAB at increasing time intervals for systems S_1 (A), S_2 (B), and S_4 (C) (see Table 1). Sampling time is indicated. Reprinted with permission from Muraviev et al. (35). Copyright [1994] American Chemical Society.

and S_5 (biphase analogs of S_2), the aqueous phase is eliminated to use only the $SO_3^-D^+$ groups and D_2O taken up by the swollen resin as a source of deuterons. System S_6 aims to elucidate the effect of trimethylamine (TMA) on both hydrolysis of TMAB and H-D exchange reaction.

Figure 1 shows typical FTIR spectra of organic phase containing TMAB at increasing time intervals for systems S_1, S_2, and S_4 (see Table 1). As seen, the FTIR technique provides a convenient mode to follow up the isotope-exchange reaction under study. For example, comparison of the spectra shown in Fig. 1 demonstrates that the deuterated product (TMAB-d_3) is formed in higher concentration in systems 2 and 4 than in system 1 (see Table 1). The quantitative expressions in terms of TMAB and TMAB-d_3 concentrations of the data presented in Fig. 1 was achieved by aid of calibration curves for TMAB solutions obtained by integrating either one band at a frequency of 2372 cm^{-1} or three bands at frequencies of 2372, 2318, and 2273 cm^{-1} (35). From the concentrations of TMAB and TMAB-d_3, the TMAB conversion (deuteration) degree F_c is calculated as follows:

$$F_c = \frac{[\mathrm{TMAB-d_3}]_t}{[\mathrm{TMAB}]_o} \tag{5}$$

where $[\mathrm{TMAB\text{-}d_3}]_t$ is the concentration of TMAB-d_3 observed at a moment t, and $[\mathrm{TMAB}]_o$ is the initial concentration of TMAB (0.1 mol/dm^3). Note that $1 \geq F_c \geq 0$.

The kinetic curves of H-D exchange and hydrolysis of TMAB obtained in systems S_1–S_6 are shown in Figs. 2–7, respectively, where respective F_c and/or F_H versus time dependencies are presented. The main parameters of TMAB deuteration process determined by studying systems S_1–S_6 are collected in Tables 2 and 3.

As seen from Fig. 2, the rate of deuteration observed in system 1 is fast, but vigorous contact of TMAB with the acidic aqueous phase promotes hydrolysis and substantially decreases the yield of TMAB-d_3. As follows from Fig. 3, a and b (see curves A), complete conversion of TMAB to TMAB-d_3 in system 2 is slower than in the case of S_1 (cf. curve A in Fig. 2). As seen in Fig. 3b, the deuterated TMAB is stable and is not readily hydrolyzed. The hydrolysis of TMAB-d_3 in this system is characterized by a time lag (see curves C and D). This simplifies operational conditions for the recovery of the product from the reaction mixture with a reasonably high yield.

Unlike biphase liquid-liquid system 1, the features of kinetics of H-D exchange in triphase systems S_2 and S_3 are mainly determined by the presence of the

Table 2. Main Parameters of TMAB Deuteration Process in Applying Liquid and Solid Deuterating Agents

System (see Table 1)	No. of Phases	Type of System (see Table 1)	Maximum Conc. of TMAB-d_3 Observed, mol/dm^3	Time of Half-Conversion ($t_{0.5}$), min	Degree of TMAB Hydrolysis Observed in $t_{0.5}$, %
S_1	2	O/A	0.070	23	15
S_2	3	O/A/R	0.088	81	9
S_3	3	O/A/R	0.081	63	7
S_4	2	O/-/R	0.100	45	<1
S_5	2	O/-/R	0.075	28	13
S_6	3	O/A/R	0.083	670	13

Reprinted with permission from Muraviev et al. (35). Copyright [1994] American Chemical Society.

Table 3. Effective Rates of H-D Exchange (R_{IE}) and Hydrolysis of TMAB (R_H) in Applying Sulfonate Cation Exchangers in D-form as Deuterating Agents

System (see Table1)	Type of Phases	Time Interval (min)	$^{*}R_{IE} \times 10^4$, s^{-1}	$^{**}R_H \times 10^4$, s^{-1}	R_{IE}/R_H	Remarks
S_2	O/A/R	$0 < t < 5$	0.2	0.5	0.4	40–60 mesh
		$5 < t < 15$	0.7	0.4	1.8	
		$15 < t < 60$	1.8	0.2	9.0	
		$60 < t < 350$	0.2	0.02	10.0	
S_3	O/A/R	$0 < t < 5$	0.7	0.3	2.3	200–400 mesh
		$5 < t < 15$	1.35	0.2	6.8	
		$15 < t < 60$	1.5	0.2	7.5	
		$60 < t < 140$	0.7	0.08	8.8	
S_4	O/-/R	$0 < t < 5$	2.9			40–60 mesh; no D_2O or D_2SO_4
		$0 < t < 15$	2.7			
S_6	O/A/R	$0 < t < 15$	0.64	0.56	1.1	40–60 mesh + TMA
		$15 < t < 100$	0.23	0.14	1.6	
		$100 < t < 365$	0.09	0.03	3.0	

* $R_{IE} = dF_c/dt$; ** $R_H = dF_H/dt$. Reprinted with permission from Muraviev et al. (35). Copyright [1994] American Chemical Society.

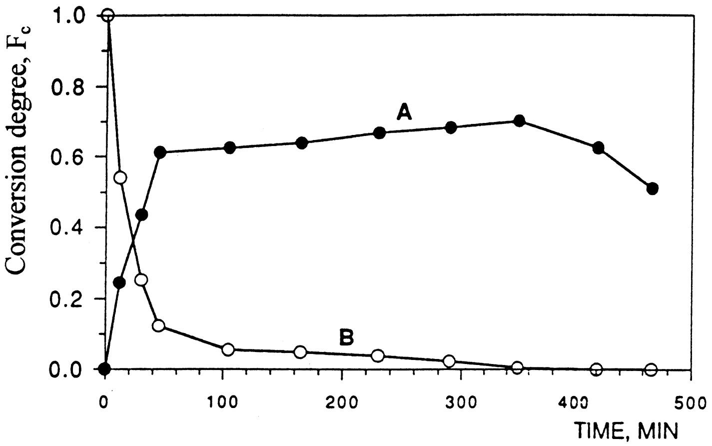

Figure 2. Kinetics of H-D exchange on TMAB in the presence of 1.6 M D_2SO_4 in biphase system S_1. Curve A corresponds to BD_3 conversion; curve B corresponds to BH_3 conversion. Reprinted with permission from Muraviev et al. (35). Copyright [1994] American Chemical Society.

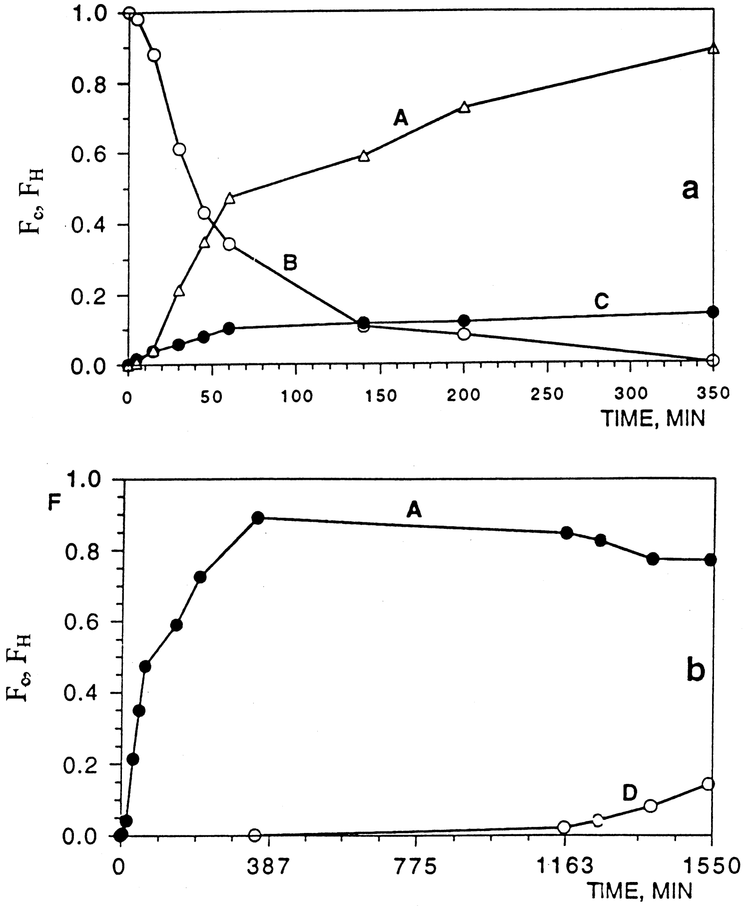

Figure 3. Kinetics of H-D exchange (curves A and B) and of hydrolysis of TMAB-TMAB-d_3 mixture (curve C) and of pure TMAB-d_3 (curve D) in the presence of Dowex 50 × 2 in D-form in triphase system (system 2). Kinetic curves are shown for time intervals: 350 min (a), 1550 min (b), corresponding to BD_3 conversion (curve A) and to BH_3 conversion (curve B). Reprinted with permission from Muraviev et al. (35). Copyright [1994] American Chemical Society.

solid resin phase in the reaction mixture. As seen in Fig. 3a, curve A is characterized by three clearly distinguished kinetic steps corresponding to $0 < t_1 < 15$-min, $15 < t_2 < 60$-min, and $60 < t_3 < 350$-min time intervals. The first and the third steps are slow, and the second is rather fast. Curve C is segmented into two parts, corresponding to the fast and slow kinetic steps of the TMAB hydrolysis, respectively, and besides, the inflection point on curve C coincides with that on curve A, corresponding to $t = 60$ min. This indicates that both isotope-exchange and hydrolysis processes are coupled and influence each other, at least in the triphase systems S_2 and S_3. This conclusion becomes clearer after a more detailed examination of the results obtained in system S_2 that makes it possible to note the following processes taking place.

(1) Hydrolysis: $0 < t < 5$ min. Rather fast primary hydrolytic decomposition of the initial TMAB proceeding according to Eq. (2) promotes the accumulation of TMA ions in the aqueous phase. TMA ions are known to increase the hydrolysis of TMAB (see below and (37)) by acting as phase-transfer catalysts (39,40). On the other hand, they can be sorbed by the resin phase with release of deuterons:

$$\text{R-SO}_3^-\text{D}^+ + (\text{CH}_3)_3\text{N}^+\text{D} \Rightarrow \text{R-SO}_3^-\text{N}^+\text{D}\,(\text{CH}_3)_3 + \text{D}^+ \qquad (6)$$

(2) Isotope Exchange: $5 < t < 60$ min. The ion-exchange reaction (6) results in simultaneous removal of TMA ions from the aqueous phase, and in the enrichment of this phase with deuterons. The first process leads to the progressive decrease in the rate of TMAB hydrolysis, and the second enhances the rate of isotope-exchange reaction, now reaching the maximum value. It is important to emphasize that this particular kinetic stage reflects the main feature of H-D exchange process proceeding in triphase systems involving solid deuterating agents (cation-exchange resins in the D-form). This feature can be defined as dual functionality of these agents acting both as *catalysts of the target process and inhibitors towards undesired side reaction*.

(3) Inhibition: $60 < t < 350$ min. Finally, the gradual loading of the cation exchanger with TMA begins inhibiting the ion-exchange process. This inhibition is explained by the surface activity of TMA ions, which resemble the cationic surfactants, known to slow down the process of ion exchange (see below) and even poison resins (38,41).

In the case of system 3 (see Fig. 4), the trends in changing the rates of isotope-exchange and hydrolysis reactions follow the same "scenario" as for S_2, i.e., first the rate of H-D exchange increases and then slows down while a permanent decreasing rate of hydrolysis is observed (see Table 3). At the same time, the rate of isotope-exchange reaction in S_3 is far higher than in S_2. This conclusion evidently follows from respective $t_{0.5}$ (time of half-conversion) and R_{IE} values ($R_{IE} = F_c/dt$) shown in Tables 2 and 3, respectively. For example, the ratio of effective rates of isotope-exchange reaction for both systems (see Table 3) at the final stage ($t > 60$ min), when the H-D exchange is considered to be a steady-state process, is $R_{IE}(S_3):R_{IE}(S_2) = 3.5$. As triphase systems S_2 and S_3 can

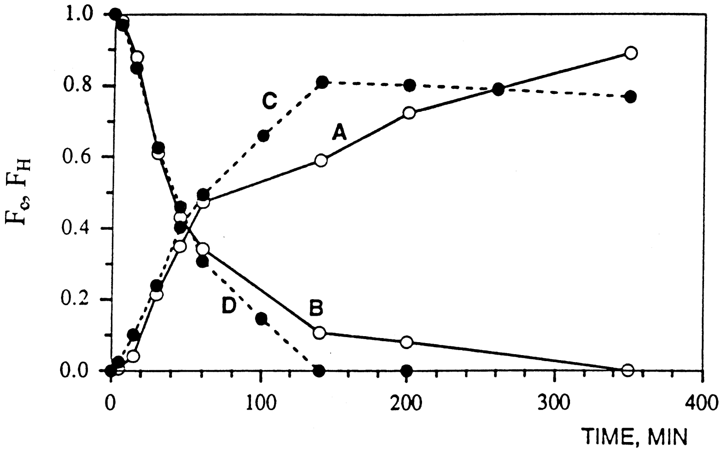

Figure 4. Kinetics of TMAB deuteration in triphase systems 2 (curves A and B) and 3 (curves C and D). Curves A and C correspond to BD_3 conversion; curves B and D correspond to BH_3 conversion. Reprinted with permission from Muraviev et al. (35). Copyright [1994] American Chemical Society.

be classified as triphase catalytic systems (42,43), the difference in the reaction rates observed can be evidently attributed to the difference in the resin sample surface areas.

The ratio of the resin surface areas in S_2 and S_3 can be estimated as follows: the number of resin beads (N_b) in each sample is equal to

$$N_b = \frac{3m}{4\pi\,\rho\, r_d^3} \tag{7}$$

where m is the mass of the resin sample (g), r_d is the average radius of the dry beads (cm), and ρ is the density of the dry ion exchanger (g/cm^3). The values of m and ρ are approximately the same for both resin samples. Hence, N_b values differ from each other because of the difference in r_d values. The surface area (S) of a given resin sample in the swollen state is equal to

$$S = 4\pi N_b r_{sw}^2 \tag{8}$$

Here r_{sw} is the average radius of swollen beads (cm), since $r_{sw} = r_d \times K_{sw}$ where K_{sw} is the linear swelling coefficient, known to depend on the resin cross-linkage. Finally one obtains

$$S = \frac{3mK_{sw}^2}{r_d\rho} \tag{9}$$

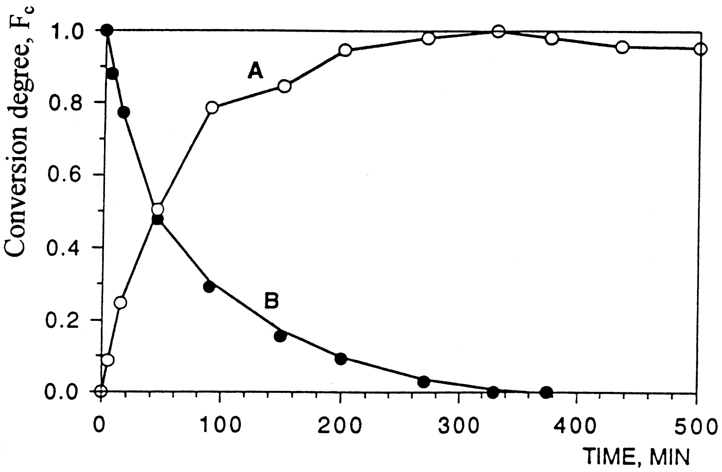

Figure 5. Kinetics of H-D exchange on TMAB in biphase system including Dowex 50 × 2 in D-form (system 4) corresponding to BD_3 conversion (curve A) and to BH_3 conversion (curve B). Reprinted with permission from Muraviev et al. (35). Copyright [1994] American Chemical Society.

and the ratio of the surface areas in S_2 and S_3 is equal to

$$S(S_3){:}S(S_2) = \frac{K_{sw3}^2 r_{d2}}{K_{sw2}^2 r_{d3}} \tag{10}$$

where the numbers in subscript refer to the number of the system under consideration. Taking into account the ratio of swelling coefficients for resins with 2 and 8% of cross-linking (known to be ~1.3 (44) and the ratio of the average radii of resin beads used ($r_{d2}:r_{d3} \approx 6$), finally one obtains $S(S_3):S(S_2) \approx 3.5$.

The above feature of H-D exchange reaction with the use of solid (polymeric) deuterating agents becomes far clearer when considering the kinetic conversion curves obtained in the biphase system 4 (see Table 1) shown in Fig. 5. As seen, in this system the concentration of TMAB-d_3 after complete conversion of BH_3 to BD_3 groups is equal to the initial concentration of TMAB (see Table 2). This indicates complete suppression of the hydrolytic decomposition of both TMAB and TMAB-d_3. The last conclusion is also confirmed by complete absence of gas evolution during the series of experiments carried out with S_4. The ^{11}B NMR analysis of the final product obtained in S_4 demonstrated the formation of spectroscopically pure $(CH_3)_3NBD_3$.

As seen from the data shown in Table 3, the effective rate of isotope-exchange reaction in system 4 is higher than in S_3, despite lower resin surface area (i.e., larger resin bead size). The shape of the kinetic curve of isotope exchange (curve A in Fig. 5) in S_4 differs from that obtained in S_2 and S_3 (cf. curves A and

C in Fig. 4). This signifies that the mechanism of H-D exchange in system 4 does not involve the kinetic steps described above. As the isotope-exchange reaction on TMAB in S_4 can proceed in the resin phase only, it must be preceded by sorption of TMAB by the ion exchanger. The most probable mechanism in this case may be dealt with the fixation of TMAB molecules on functional groups of the ion exchanger, simplifying their transfer (in sorbed state) into the transition complex and finally into TMAB-d_3. The overall exchange reaction can be described by the following scheme:

$$\overline{(CH_3)_3NBH_3} + R - SO_3^- \, {}^+D_3O \rightarrow \overline{(CH_3)_3NBD_3} + R - SO_3^- \, {}^+H_3O \quad (11)$$

where R denotes the resin phase and the bar over TMAB indicates its presence in the resin phase. Since the resin phase is a low-cross-linked ion exchanger preswollen in D_2O it contains a considerable amount of deuterium oxide (see below). This creates the conditions for "self-regeneration" of the exhausted part of the ion exchanger by the following reaction:

$$R(SO_3^- \, {}^+H_3O + 1.5D_2O \rightarrow R - SO_3^- \, {}^+D_3O + 1.5H_2O \quad (12)$$

The confirmation of the self-regeneration mechanism was obtained in the series of experiments on sequential treatment of four portions of a 0.1 M TMAB solution with the same portion of Dowex 50 × 2 in the D-form (5.2 mEq) in S_4-like systems (45). The results obtained in this series of experiments are shown in Fig. 6 and in Table 4. The effective rates of H-D exchange reaction ($R_{IE} = dF_c/dt$)

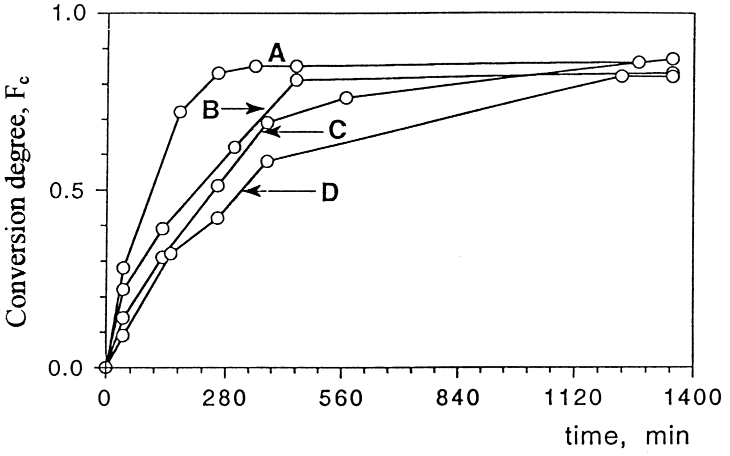

Figure 6. Kinetic curves of TMAB-d_3 formation in sequential treatment of four portions of 0.1 M TMAB solution: 1st (A), 2nd (B), 3rd (C), and 4th (D) with sample of Dowex 50 × 2 in D-form. Reprinted from Muraviev and Warshawsky (45), reprinted with permission from Elsevier Science.

Table 4. Effective Rates of H-D Exchange (R_{IE}) in Sequential Deuteration of Four Portions of 0.1 M TMAB Solution in Applying the Same Sample of Sulfonate Cation Exchangers in D-Form as Deuterating Agent

Sample No.	Volume of TMAB Solution (cm^3)	F_c	TMAB-d_3 Obtained (mmol)	D_2O Reacted (mmol)	$R_{IE} \times 10^4$ (s^{-1})
1	20.0	0.86	1.72	2.58	1.17
2	30.0	0.83	2.49	3.74	0.91
3	20.0	0.87	1.74	2.61	0.61
4	20.0	0.82	1.64	2.46	0.37

Reprinted from Muraviev and Warshawsky (45) with permission from Elsevier Science.

collected in Table 4 (see last column) were calculated from the initial slopes of the kinetic curves shown in Fig. 6. The initial resin phase content of D_2O ($Q_{o,sw}$, mmol), representing the amount of D_2O taken up by the swollen polymer, can be calculated as follows:

$$Q_{o,sw} = \frac{V(1-\varepsilon)W}{\rho M} \tag{13}$$

where V is the volume of the resin sample in cm^3 (3.8 cm^3 measured as a compact bed); W is the fraction of the water content in the swollen resin (~80% for Dowex 50 × 2 (44); $M = 20$ g/mol (the molecular mass of D_2O), and $\rho = 1.105$ g/cm^3 (the density of D_2O). Estimation of $Q_{o,sw}$ value by using Eq. (13) gives a value of ~90 mmol, which is considerably higher than the full ion-exchange capacity of the resin sample (5.2 mEq). The amounts of D_2O reacted in every run of the kinetic experiment (see Table 4) were calculated according to the stoichiometry of the following equation obtained by summarizing Eqs. 11 and 12:

$$\overline{(CH_3)_3NBH_3} + 1.5D_2O \xrightarrow{R-SO_3^-\,{}^+D_3O} \overline{(CH_3)_3NBD_3} + 1.5\,H_2O \tag{14}$$

These values allow the estimation of unreacted amounts of D_2O in the resin phase ($Q_{sw}(D_2O)$) as the remainder after consequentially subtracting the figures given in the fifth column of Table 4 from $Q_{o,sw} = 90$ mmol. The plot of effective rates of the H-D exchange (see R_{IE} values in Table 4) versus $Q_{sw}(D_2O)$ is shown in Fig. 7. As seen, the R_{IE} versus $Q_{sw}(D_2O)$ dependence is satisfactorily approximated by a straight line. This indicates that reaction 14 is of the pseudo-first order in D_2O and confirms the self-regeneration mechanism proposed.

The overall amount of TMAB-d_3 obtained in this series of experiments is equal to ~7.6 mmol (see Table 4), which substantially exceeds the full ion-exchange capacity of the resin sample used (5.2 mEq). This confirms the above conclusion that deuteriosulfonic acid groups of the ion exchanger act as a catalyst (or transfer agent) in the isotope-exchange reaction.

The self-regeneration of the resin (see above) appears to play a key role in the proposed mechanism. The equilibrium in reaction 12 can be expected to be shifted to the right because of the difference in the value of dissociation constants of proto (pK_H) and deutero acids (pK_D) (46–48). For example, the difference in the second dissociation constants for H_2SO_4 and D_2SO_4 is $\Delta pK = pK_D - pK_H = 0.30$ (46,47). Similar or even higher ΔpK values can be expected for the sulfonic acid groups of an ion exchanger.

The preparation of the resin in the D-form involves the use of sufficiently concentrated solution of D_2SO_4, which can be sorbed by the resin phase by the Donnan invasion mechanism (44,49). The influence of sorbed D_2SO_4 on the kinetics of both isotope exchange and hydrolysis reactions carried out with system 5 (see Table 1) is shown in Fig. 8. The comparison of the data presented in Fig. 5 with that shown in Fig. 8 allows the conclusion that presence of D_2SO_4 in the resin phase significantly intensifies the hydrolytic decomposition of both TMAB and TMAB-d_3 and decreases the yield of the final product (see Table 2). This confirms the importance of the removal of sorbed acid from the resin prior to its use in the isotope-exchange reaction.

The confirmation of the kinetic mechanism proposed above is seen in Fig. 9 where the kinetics of H-D exchange and hydrolysis of TMAB in system 6 (see Table 1) is shown. Indeed, as follows from the comparison of the data given in

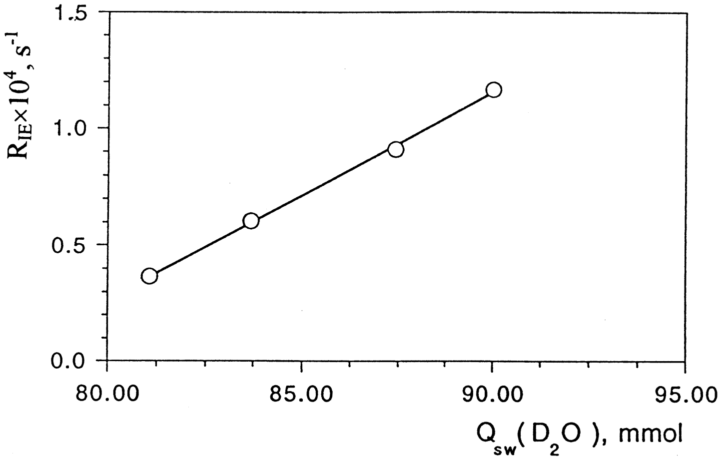

Figure 7. Effective rate of H-D exchange on TMAB (R_{IE}) plotted versus amount of unreacted D_2O in resin phase (see Table 4). Reprinted from Muraviev and Warshawsky (45), with permission from Elsevier Science.

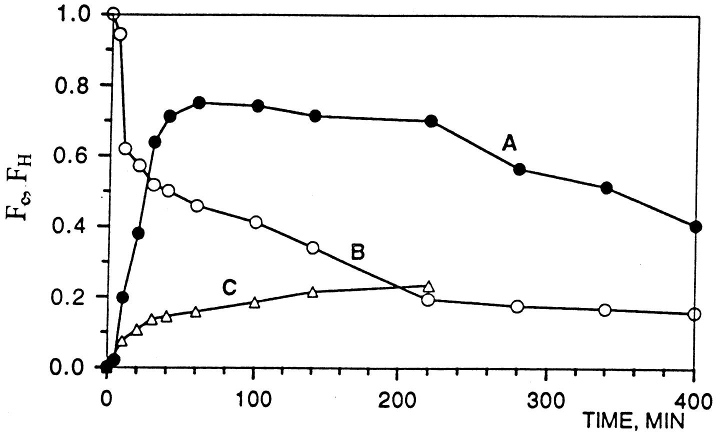

Figure 8. Kinetics of H-D exchange (curves A and B) and of hydrolysis of TMAB-TMAB-d_3 mixture (curve C) in biphase system including Dowex 50 × 2 in D-form with sorbed D_2SO_4 (system 5). Curve A corresponds to BD_3 conversion; curve B corresponds to BH_3 conversion. Reprinted with permission from Muraviev et al. (35). Copyright [1994] American Chemical Society.

Fig. 9 with that shown in Fig. 3 the presence of TMA in the aqueous phase subsequently slows down the isotope-exchange reaction due to the gradual loading of the resin phase with TMA ions. On the other hand, sorption of TMA decreases its concentration in the aqueous phase and also slows down the hydrolysis of TMAB.

The results obtained by a more detailed study of the hydrolysis of TMAB have led to the following important practical conclusions on the active role of TMA in the process under consideration (37):

1. TMA may be used as a "rate regulator" for both hydrolytic and isotope-exchange reactions of TMAB in systems involving liquid (mineral) or solid (polymeric) acids.
2. The nitrogen-bound hydrogen ions (deuterons or protons) of TMA salts do not exchange with hydride hydrogens of TMAB or any other borohydrides. This has been confirmed by Kampel and Warshawsky, who successfully synthesized monoisotopic amine trideuterioborane adducts using commercial trialkylamine hydrochloride without any special pre-treatment (34).

The comparison of effective rates of isotope exchange (R_{IE}) and of hydrolysis (R_H) in the most interesting systems (S_2, S_3, S_4, and S_6, see Table 1) is summarized in Table 3 where R_{IE} and R_H values at different reaction time zones are presented. The ratio R_{IE} to R_H shows the selectivity of the reaction steps. At the initial time interval ($0 < t < 5$ min) the hydrolysis reaction is favored, but this changes with time. Higher selectivities for the isotope-exchange reaction are observed after a longer time ($t > 5$ min) for all systems. Reduction of the triphase systems (S_2 or S_3) to a corresponding biphase one (S_4) by exclusion of the liquid aqueous phase (D_2O) ensures almost indefinitely high selectivity for the isotope-exchange reaction.

This is a manifestation of a state where the water is actually immobilized in the swollen polymer, in contrast to an organic solution of the reactant. From this viewpoint, the systems of S_4 type, known in the literature as aqua impregnated resins (AIR) (44,49–51) can be compared with extraction chromatographic material (ECM) or solvent impregnated resin (SIR) models (53–61). Such a comparison is shown schematically in Fig. 10 (61). As seen, immobilization of the aqueous component of an extraction system in a polymeric phase (e.g., in ion-exchange resin) to form an AIR may be considered as a "symmetrical reflection" of the ECM-SIR concept. Note that the "symmetry" of corresponding AIR and SIR systems is observed when immobilization of a liquid component of a liquid-liquid extraction system is not accompanied by any chemical interactions between immobilized component and solid support (50). Besides a number of advantages resulting from conversion of a liquid-liquid into a solid-liquid extraction system, in the present case such a conversion allows (1) complete suppression of TMAB

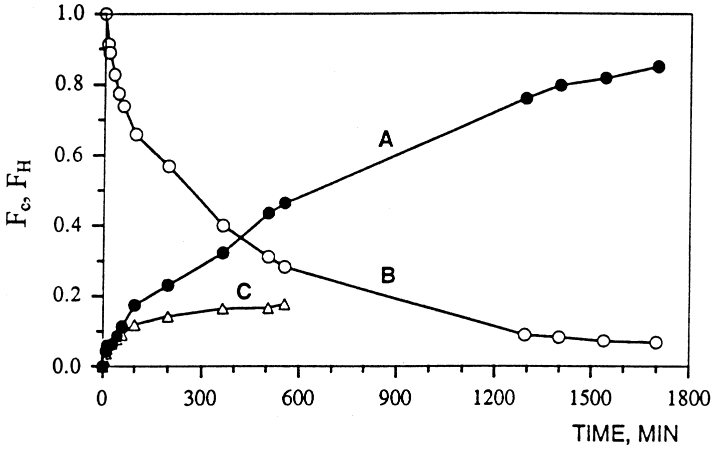

Figure 9. Kinetics of H-D exchange (curves A and B) and of hydrolysis of TMAB-TMAB-d_3 mixture (curve C) in triphase system including Dowex 50 × 2 in D-form and 0.14 M solution of trimethylamine deuterosulfate in D_2O (system 6). Curve A corresponds to BD_3 conversion; curve B corresponds to BH_3 conversion. Reprinted with permission from Muraviev et al. (35). Copyright [1994] American Chemical Society.

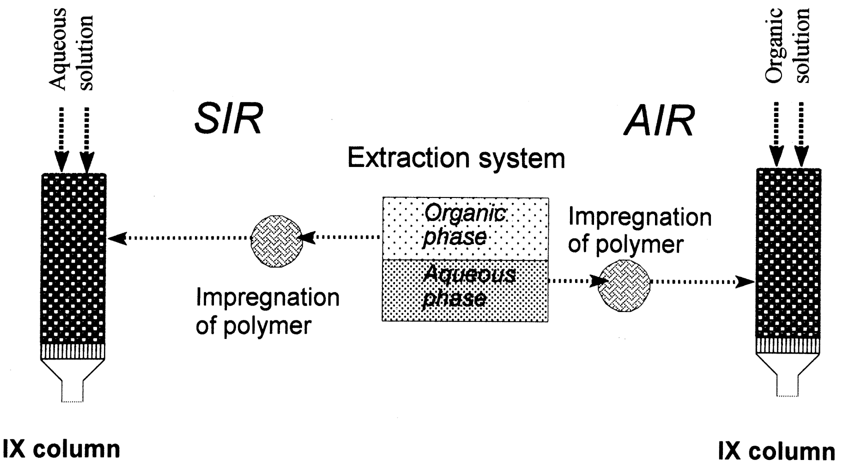

Figure 10. Comparison of ECM-SIR and AIR concepts.

hydrolysis, and (2) permits the use of convenient dynamic mode of operation in an ion-exchange column.

CONVERSION OF TMAB TO TMAB-D$_3$ IN ION-EXCHANGE COLUMN

The H-D exchange process was carried out under dynamic conditions by using an ion-exchange column loaded with Dowex 50 × 2 resin (resin bed height of ca. 5 cm, inner diameter of the column = 0.46 cm) by following the procedure described elsewhere (45). After converting the resin into the D-form and washing out the sorbed D_2SO_4 with D_2O the resin bed was equilibrated with CCl_4 by passing several bed volumes of pure CCl_4 through the column. Then the 0.1 M TMAB solution in CCl_4 was passed through the resin bed at a constant flow-rate of 0.1 cm^3/min and collected in portions. The concentration of both TMAB and TMAB-d$_3$ were determined in all samples by FTIR analysis following the disappearance of the strong B-H absorption band at 2360 cm^{-1} and appearance of the broad B-D band at 1783 cm^{-1}.

A typical volume-concentration history obtained in this version of the TMAB deuteration process after the first run of initial TMAB solution is shown in Fig. 11. The numbered dots in Fig. 11 denote the eluate portions for which FTIR spectra are shown in Fig. 12. As it is clearly seen in Fig. 12, a gradual decrease of the BH_3 peak (2360 cm^{-1}) accompanied by substantial increase of the BD_3 peak (1783 cm^{-1}) are observed as the H-D exchange proceeds. The enrichment coeffi-

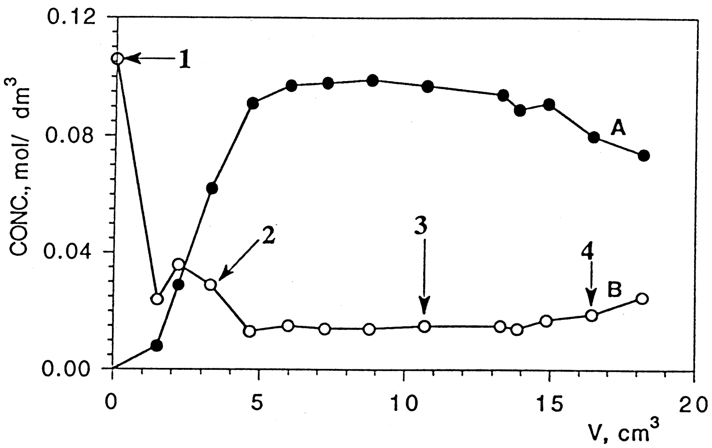

Figure 11. Effluent-concentration history of H-D exchange on TMAB in column containing Dowex 50 × 2 in D-form (1st elution of 0.1 M TMAB in CCl_4). Curves A and B correspond to TMAB-d_3 and TMAB, respectively. Numbered dots indicate solution samples for which FTIR spectra are shown in Fig. 12 (V is volume). Reprinted from Muraviev and Warshawsky (45), with permission from Elsevier Science.

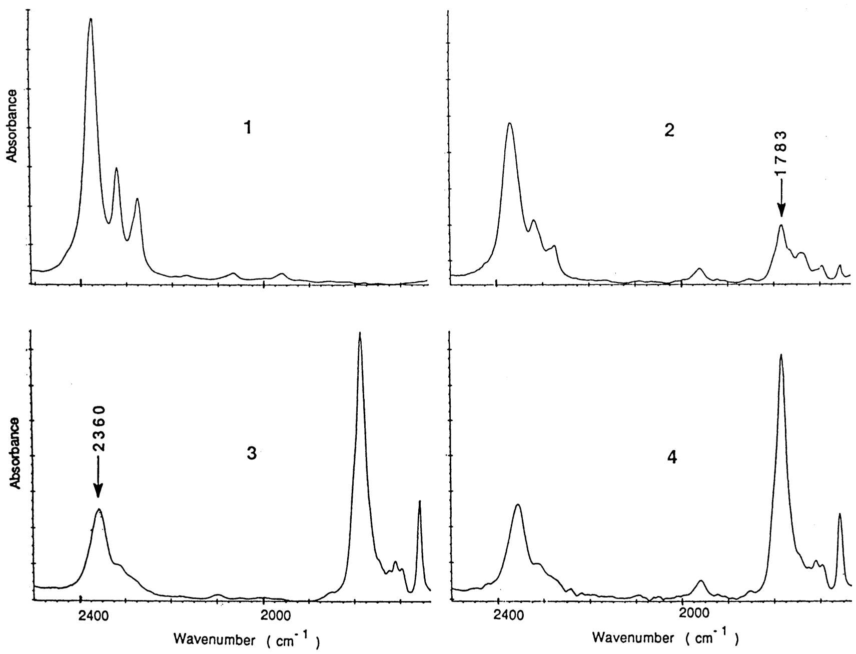

Figure 12. FTIR spectra of samples taken at points 1–4 of curve B in Fig. 11. Reprinted from Muraviev and Warshawsky (45), with permission from Elsevier Science.

cients (C_E) can be calculated from the concentrations of TMAB and TMAB-d_3 in the respective eluate samples as follows:

$$CE = \frac{[\text{TMAB} - d_3]_i}{[\text{TMAB}]_i} \tag{15}$$

The elution curve shown in Fig. 11 is reproduced in Fig. 13 in terms of C_E values. Comparison of the breakthrough curves presented in Figs. 11 and 13 shows that, despite the non-monotonous character of the initial part of the TMAB elution curve (see curve B in Fig. 11), a smooth increase of C_E values is observed (see Fig. 13), followed by a plateau range characterized by practically constant C_E values. Then a decrease of C_E values is observed that is attributed to the gradual exhaustion of the resin bed, which causes slowing down of the H-D exchange reaction. Samples of eluate in the plateau range from several different runs were collected separately and then rerun through a column containing a fresh portion of Dowex 50 × 2 in the D-form.

A typical concentration-volume history obtained in a second elution of the TMAB-d_3-enriched TMAB-TMAB-d_3 mixture (obtained after the first run) through a fresh resin bed is shown in Fig. 14. Numbered dots in Fig. 14 indicate solution samples for which FTIR spectra are shown in Fig. 15. As seen from Figs. 14 and 15, the second treatment of TMAB solution in the column with a fresh portion of the resin in the D-form results in the formation of a zone with spectroscopically pure TMAB-d_3 (see spectrum 1 in Fig. 15). This conclusion is also confirmed by the results of ^{11}B NMR and ^{2}D NMR analysis shown in Figs. 16 and 17, respectively (see Appendix), of the initial TMAB and of TMAB-d_3 obtained from eluate samples characterized by zero absorption at a frequency of 2360 cm^{-1} (see

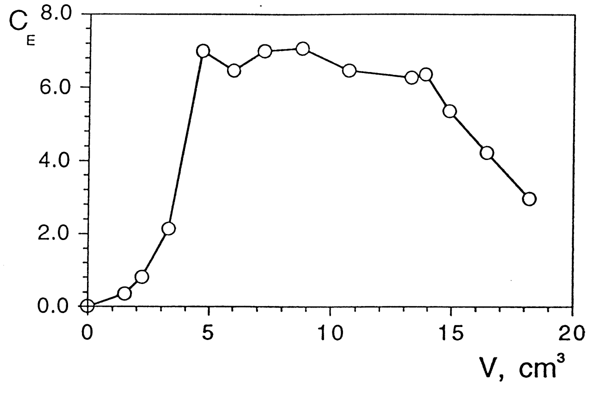

Figure 13. Reproduction of elution curve shown in Fig. 11 in terms of enrichment coefficients (C_E) values calculated from Eq. (15) (V is volume). Reprinted from Muraviev and Warshawsky (45), with permission from Elsevier Science.

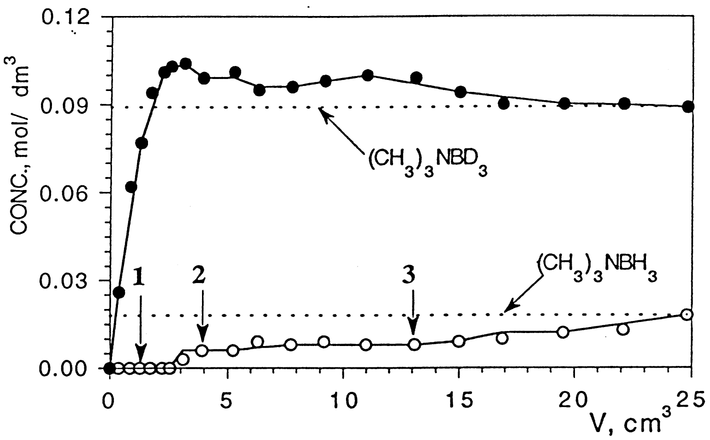

Figure 14. Effluent-concentration history of second run of TMAB (open cycles)-TMAB-d_3 (closed cycles) through Dowex 50 × 2 in D-form bed. Dotted lines denote initial content of TMAB-d_3 and TMAB species in solution under treatment. Numbered dots indicate solution samples for which FTIR spectra are shown in Fig. 13 (V is volume). Reprinted from Muraviev and Warshawsky (45), with permission from Elsevier Science.

spectrum 1 in Fig.15). As seen in Fig. 16a, ^{11}B NMR spectrum of the initial TMAB shows a quartet at −8.2 ppm, and that of the pure TMAB-d_3 (see Fig.16b) is characterized by a broad singlet at around −8.4 ppm. Note that similar spectrum was observed by the ^{11}B NMR analysis of TMAB-d_3 obtained in experiments with system 4 (see above Table 1 and Fig. 5). The ^{2}D NMR spectrum for the same TMAB-d_3 sample (see Fig.17) shows a broad doublet centered at 1.8 ppm.

As it clearly follows from Fig. 14, the pure deuterated product can be easily recovered from separately collected portions of eluate corresponding to the head part of breakthrough curve. The rest of the eluate samples (additionally enriched by TMAB-d_3) can be repeatedly treated in a column with a fresh portion of the resin in the D-form to produce the second portion of completely deuterated product, etc. Due to the absence of hydrolytic decomposition of TMAB and TMAB-d_3 in the AIR deuteration system under consideration the total yield of the final product can be as high as 100%.

To conclude this section it seems important to emphasize that the proposed column technique gives a unique opportunity to obtain 100% pure deuterated product within several hours of work versus 240 h in the case of the procedure described by Atkinson et al. (7,8). Furthermore, if in the case of liquid-liquid extraction the exhausted solution of the deuterating agent cannot be regenerated and must be replaced with a fresh one, the polymeric deuterosulfuric acid (Dowex 50 × 2 in the D-form) can be easily reused after exhaustion. The resin regeneration

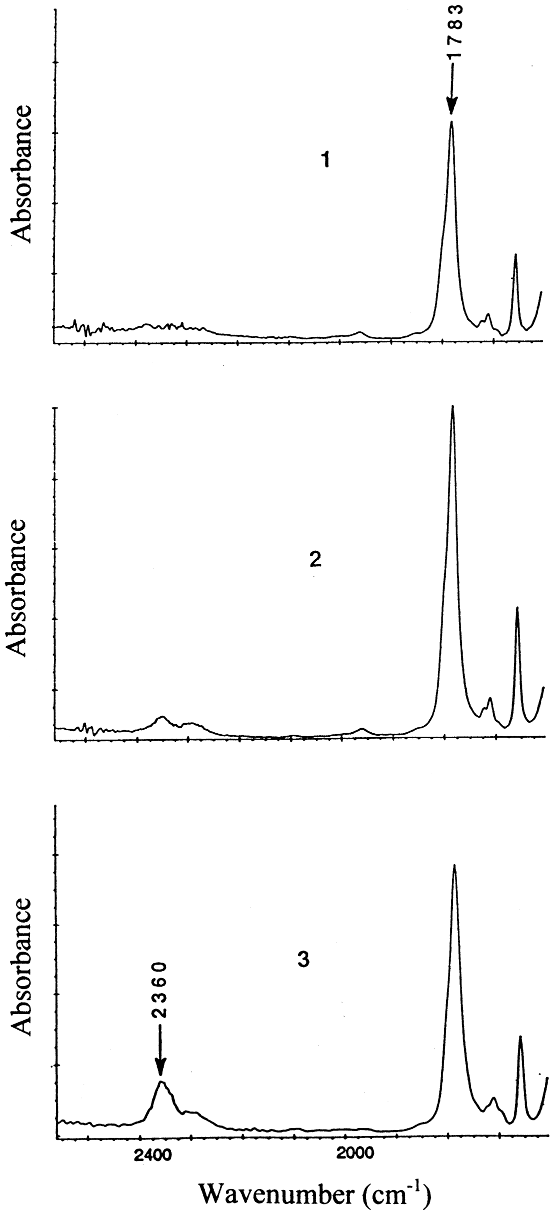

Figure 15. FTIR spectra of samples taken at points 1–3 of TMAB elution curve in Fig. 14.

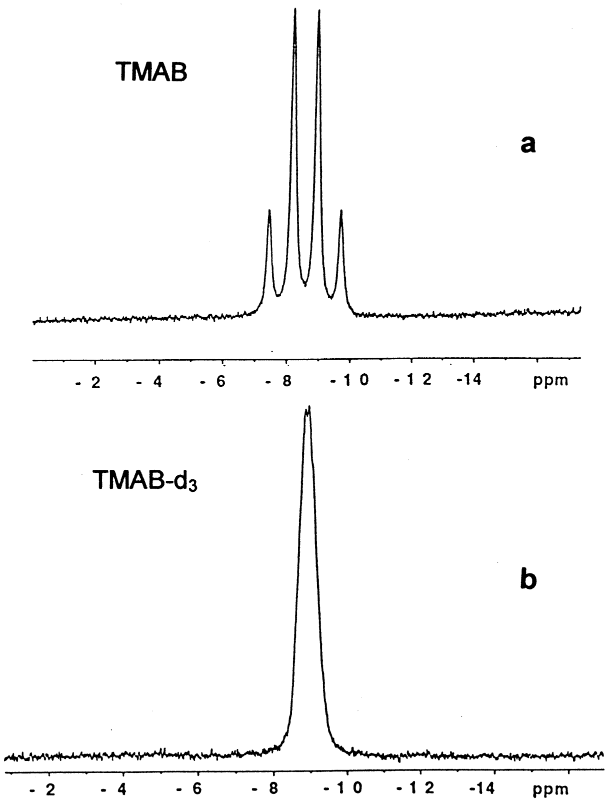

Figure 16. ^{11}B NMR spectra of TMAB (a) and TMAB-d_3 (b) obtained from eluate samples with zero absorption at 2360 cm^{-1} (see Figs. 14 and 15).

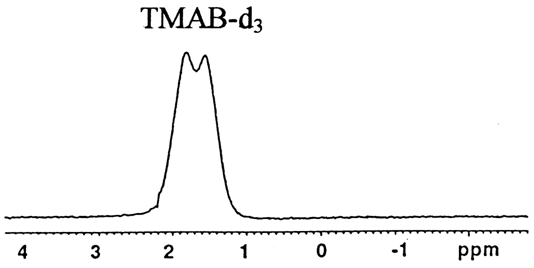

Figure 17. ^{2}D NMR spectrum of TMAB-d_3 obtained from eluate samples with zero absorption at 2360 cm^{-1} (see Figs. 14 and 15).

stage may include either rinsing the resin in a column with D_2O or subsequently drying the ion exchanger and placing it in D_2O to swell. In both cases the H_2O admixture (appearing in the polymer according to Eq. 12) will be removed. All these operations can be achieved in the same ion-exchange column starting from the preparation of the ion exchanger in the deutero form and up to production of pure deuterated product.

MEMBRANE-ASSISTED TMAB DEUTERATION PROCESS

Another AIR-like system that can be used to carry out the H-D exchange reaction on TMAB is a membrane reactor (MR) supplied with a cation-exchange membrane in the D-form. A two-compartment ion-exchange MR shown schematically in Fig. 18b can be considered to be something in between a tri-phase system of S_2-type and a S_4-like biphase system (see Table 1), also shown schematically in Fig. 18, a and c, respectively. Indeed, as seen in Fig. 18, a and b, in both S_2-like system and MR (which is also composed of three phases), the ion exchanger phase (granulated resin in S_2 and plane membrane in MR) is in contact with both liquid phases (aqueous and organic). On the other hand, in both MR and S_4-like systems the organic phase is contacting with the ion exchanger phase only. The functionality of the ion-exchange resin in S_2 and S_4 is similar to that of the ion-exchange membrane used in MR experiments. This suggests a similarity of mechanisms of both H-D exchange and TMAB hydrolysis reactions (see above) proceeding in systems under comparison. Hence, the TMAB deuteration process when carried out in an MR can also be expected to proceed by some "intermediate" rout. In other words, the features of H-D exchange reaction in an MR must be similar to those of TMAB deuteration in both S_2 and S_4 depending on the experimental conditions.

The MR-version of TMAB deuteration process was studied by using the sealed membrane cell as described in detail elsewhere (62,63). The feed compart-

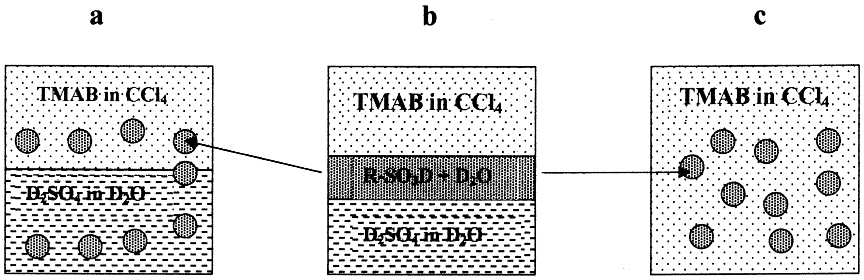

Figure 18. Comparison of membrane reactor (b) with triphase systems of S_2 or S_3 type (a) and biphase system S_4 (c). See Table 1.

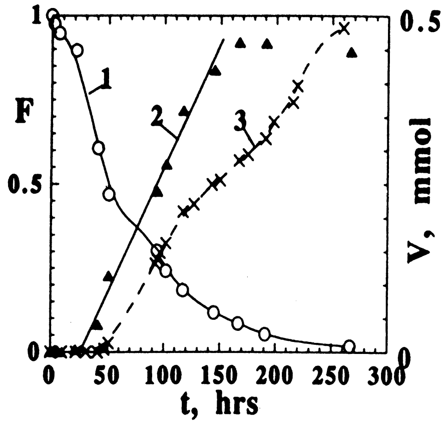

Figure 19. Degree of conversion of TMAB (curve 1) and of TMAB-d_3 (curve 2) in MR as function of time. Curve 3 shows kinetics of gas evolution from feed aqueous phase. Initial conditions: $[TMAB]_o = 0.2$ M; $[D_2SO_4]_o = 72$ mM. Reprinted with permission from Bromberg et al. (62). Copyright [1993] American Chemical Society.

ment of the cell was filled with a solution of D_2SO_4 in deuterium oxide and the receiver section with a solution of TMAB in carbon tetrachloride. The volumes of both reactor compartments were equal to 15 cm^3. The cation-exchange membrane composed of highly sulfonated polyethylene (purchased from Soreq Nuclear Research Center, Israel), with an operating area of 3.14 cm^2 was preliminary equilibrated with the feed solution of a given composition before use in MR. The progress of the H-D exchange reaction was followed by volumetric, FTIR, and ^1H and ^{11}B NMR analyses (see above and Appendix).

The typical results obtained in the MR kinetic experiments are shown in Fig. 19. As seen, at a relatively high TMAB concentration (0.2 mol/dm^3) the behavior of the system resembles that of S_2 and S_3 (see above and Figs. 3 and 4). Indeed, the concentration of TMAB gradually decreases (see curve 1) and the TMAB-d_3 concentration increases after a certain time lag Δt_1, reaches a maximum, and then decreases. The value of Δt_1 is obviously determined by the rate of D_2SO_4 diffusion through the membrane. Volumetric data demonstrated no gas evolution from the organic receiver phase and a marked evolution of the gas from the "aqueous" feed section (see curve 3). This means that the hydrolysis of both TMAB and TMAB-d_3 occurs in the feed compartment of MR or, more exactly, at the membrane-aqueous solution interface (see Fig. 18b) while the conversion of TMAB to TMAB-d_3 occurs at the organic solution-membrane interface. Hence, unlike S_2 and S_3 systems *in MR the target and the undesired side reactions appear to be separated in space* that is of particular importance for optimization of the deuteration process. The hydrolysis of TMAB in the feed phase is also confirmed by the results of ^{1}H NMR analysis of the aqueous feed solution shown in Figs. 20 and 21. The spectrum of the feed phase (see Fig. 20) revealed water as a major component at $\delta = 4.8$ ppm and TMA sulfate as a minor component at $\delta = 3.1$ ppm. The appearance of water (see Fig. 21) is of particular importance in understanding the above-discussed mechanism of the isotope-exchange reaction.

It is interesting to note that the gas evolution (see curve 3 in Fig. 19) is also observed after a time lag (Δt_2), whose value is higher than Δt_1. Quite evidently for the hydrolysis reaction to occur both TMAB and TMAB-d_3 species must diffuse through the membrane from the receiver to the feed phase. On the other hand, the H-D reaction at the membrane-organic solution interface requires the transport of D_2SO_4 across the membrane in the opposite direction (from the feed to the receiver phase). Hence, the observed difference in Δt_1 and Δt_2 is evidently attributed to different rates of diffusion of TMAB (or TMAB-d_3) and D_2SO_4 species in the membrane. The diffusion rate of each component must, in turn, be proportional to the gradient of component concentration, ΔC_i, across the membrane, which can be defined (for the initial part of MR experiment) as follows:

$$\Delta C_i = \frac{C_{io}}{\delta} \qquad (16)$$

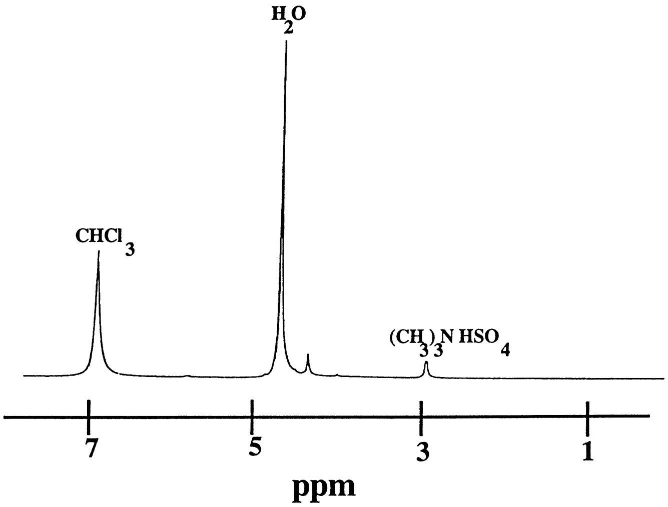

Figure 20. ^{1}H NMR spectrum of receiver phase 168 h after start of kinetic experiment shown in Fig. 19. Reprinted with permission from Bromberg et al. (62). Copyright [1993] American Chemical Society.

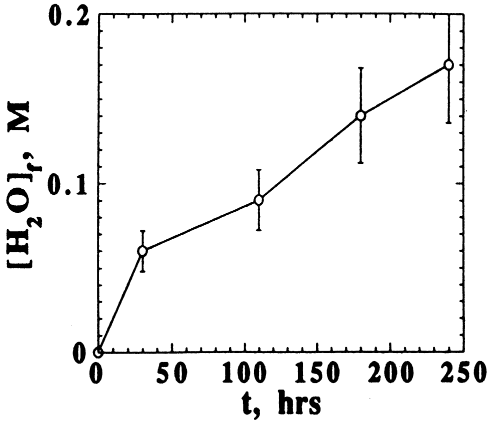

Figure 21. Kinetics of H_2O appearance in feed phase in experiment shown in Fig. 19. Reprinted with permission from Bromberg et al. (62). Copyright [1993] American Chemical Society.

where C_{io} is the initial concentration of component "i", and δ is the thickness of the membrane.

The above discussion leads to the following important conclusions:

1. Variation of the initial concentration of components in the receiver and feed phases must substantially influence the rates of reactions occurring at the corresponding membrane interfaces.
2. The decrease of the initial TMAB concentration must cause an increase of Δt_2 value resulting in a temporal deactivation of the aqueous solution-membrane interface, which is responsible for the undesired hydrolysis reaction. As the result, the TMAB-TMAB-d_3 hydrolysis must be temporally suppressed whereas the H-D reaction will not be affected.

The confirmation of the first conclusion is seen in Fig. 22, where the dependence of the isotope exchange rate constant R_{IE} on the initial concentration of D_2SO_4 in the receiver phase is shown. The substantiation of the second conclusion is clearly seen in Fig. 23. The only difference in conditions of experiments shown in Figs. 19 and 23 is a ten-time less initial concentration of TMAB in the last case. For the experiment described in Fig. 23, during 200 h, monitoring of both feed and receiver phases showed the absence of gas evolution in either of them, i.e., no hydrolysis was observed. Thus, under the conditions of this experiment the yield of TMAB-d_3 reached 100 %. After 220 h the deuterated product started to hydrolyze (see curve 3 in Fig. 23.

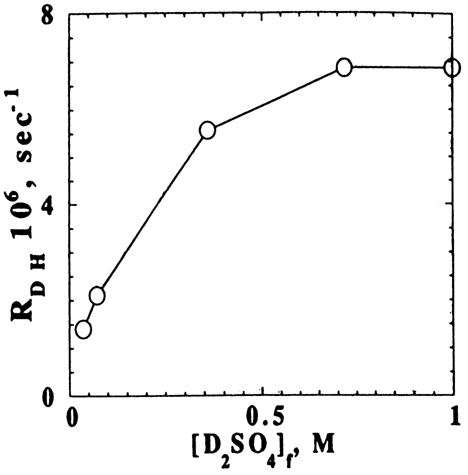

Figure 22. Dependence of R_H on initial concentration of D_2SO_4 in receiver phase. Initial conditions: $[TMAB]_o$ = 0.2 M. Reprinted with permission from Bromberg et al. (62). Copyright [1993] American Chemical Society.

A comparison of the results shown in Figs. 19 and 23 with those obtained by studying systems S_2 and S_4 (see Figs. 3 and 5) permits the following conclusion: at a relatively high initial concentration of TMAB, the deuteration process in the MR system follows the “scenario” of that in S_2. A decrease of TMAB con-

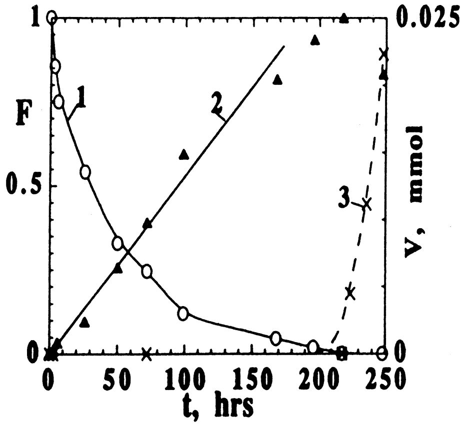

Figure 23. Degree of conversion of TMAB (curve 1) and of TMAB-d_3 (curve 2) in MR as function of time. Curve 3 shows kinetics of gas evolution from feed aqueous phase. Initial conditions: $[TMAB]_o$ = 20 mM; $[D_2SO_4]_o$ = 72 mM. Reprinted with permission from Bromberg et al. (62). Copyright [1993] American Chemical Society.

centration essentially allows for reduction of the MR system to system 4 through deactivation of the aqueous solution-membrane interface and suppression of the undesired hydrolytic decomposition of both initial substrate (TMAB) and the final product (TMAB-d_3). A substantiation of this conclusion is also provided by the comparison of the R_{IE} values determined in S_4 and the corresponding MR system. In system 4, the effective rate for H-D exchange is $2.9 \times 10^{-4}\ s^{-1}$ (see Table 3), whereas the surface area of the resin phase is $\sim 3 \times 10^2\ cm^2$ (see above). The value of the effective rates of H-D exchange in the MR systems ranged from $1.5–7.5 \times 10^{-6}\ s^{-1}$ (62), whereas the membrane surface area (operating area) was $3.14\ cm^2$. Hence, both types of AIR systems under consideration demonstrate similar intrinsic rates of isotope-exchange reaction.

CONCLUSIONS

The following main conclusions can be derived from the results presented above:

1. Solid (polymeric) cation-exchange resins in the D-form can be successfully used as novel deuterating agents with dual function permitting, on one hand, to carry out the target H-D exchange reaction at sufficiently high rate, and, on the other hand, to completely suppress the undesired side-reaction. The ion exchanger acts as a catalyst in the first reaction and as an inhibitor in the second.
2. Immobilization of the aqueous component of a liquid-liquid extraction system in a swollen polymer transforms it into an AIR (a solid-liquid system). Such immobilization allows complete suppression of TMAB hydrolysis and leads to 100% pure deuterated products in two stages by a column technique. The polymeric deuterosulfuric acid can be easily reused after exhaustion. The regeneration stage may include, e.g., either rinsing the resin with D_2O or subsequently drying the ion exchanger and placing it in D_2O to swell. This allows for convenience of preparation procedure and low cost of the final product.
3. The use of the membrane version of AIR deuteration system, representing an MR supplied with a cation-exchange membrane in the D-form adds one more advantage: it allows complete separation of the target product and side products, so that the desired deuterated product is obtained from the organic phase in the pure state. It also allows control of undesired hydrolysis by varying the concentration of TMAB so that 100% yield of TMAB-d_3 can be achieved.

APPENDIX

The ^{1}H NMR, ^{2}D NMR, and ^{11}B NMR spectra were recorded on a Bruker AMX400 spectrometer with a broad-band probe in a 5-mm NMR tube (^{1}H resonance at 400.13 MHz, ^{2}D resonance at 61.4 MHz, ^{11}B resonance at 128.4 MHz) by using a tip angle of 90° (6 μs) and a pulse repetition time of 1 s. D_2O and $CDCl_3$ was used as a frequency lock. External reference of ^{11}B spectra was made by taking the signal for boron trifluoride etherate in $CDCl_3$ at $\delta = 0.0$ ppm. Tetramethylsilane was used as a reference for the ^{2}D spectra. The series of the kinetic ^{1}H experiments with the feed phase of MR were carried out as follows: a weighted amount of the feed solution was withdrawn at a given time from the cell by using a quartz capillary (Bruker), which was placed into the NMR tube containing a preweighted amount of $CDCl_3$ to which the NMR spectrometer was locked-on. Use of known weights of $CDCl_3$ and the feed phase and calibration of the ratio of the peaks corresponding to $CDCl_3$ and H_2O provided a method of measuring the relative amount of water in the feed phase (see Fig. 21).

ACKNOWLEDGMENTS

Prof. Abraham Warshawsky is holding the Rebecca and Israel Sieff Professorial Chair in organic chemistry. A.W. acknowledges Prof. Israel Dostrovski for drawing him into the exciting work of the Gallex project and convincing him of the need to develop a unique synthesis of monoisotopic borohydrides. A.W. also thanks his coauthors in the references quoted for excellent contributions in developing the project to its successful outcome: Dr. Vladimir Kampel for synthetic contributions in Boron chemistry, Dr. Lev Bromberg for membrane work, and Ilana Rogachev for the borohydride synthesis. D.M. acknowledges a fellowship from the Israeli Ministry of Immigration and Absorption during his stay at the WIS from 1991–1993 and thanks the Spanish Ministry of Science and Education for the financial support during his Visiting Professorship at the Universitat Autónoma de Barcelona.

REFERENCES

1. Thomas, A.F. *Deuterium Labelling in Organic Chemistry*; Appleton-Century-Crofts: New York, 1971.
2. Evans, E.A. *Tritium and Its Compounds*, 2nd Ed.; Butterworth: London, 1974.
3. Buncel, E.; Lee, C.C., Eds. *Isotopes in Organic Chemistry;* Elsevier: Amsterdam, Vols. 1–5.

4. Elvidge, J.A.; Jones, J.R, Eds. *Isotopes: Essential Chemistry and Applications;* special publication No.35; The Chemical Society Burlington House: London, 1980.
5. Zimmermann, H. Liquid Crystals **1989,** *4* (6), 591.
6. Crout, D.H.; Haurahan, J.R.; Hutchinson, D.W. Carbohydr. Res. **1993**, *239*, 305.
7. Atkinson, J.G.; Tremaine, P.H. Canada Patent 762,843, 1967.
8. Atkinson, J.G.; MacDonald, D.W.; Stuart, R.S.; Tremaine, P.H. Can. J. Chem. **1967**, *45*, 2583.
9. Kampel, V.; Rogachev, I.; Warshawsky, A. Monoisotopic borohydrides. I. Synthesis of borohydrides by alkaline hydrolysis of magnesium boride. II. Preparative synthesis of sodium borohydride (T-free) by polymer catalyzed exchange on trimethylamine borane. Gallex Report No. GX-61, October, 1994.
10. Hampel, W. In *AIP Conf. Proc.*, No. 56, Heidelberg, Germany, 1983; 88–95.
11. Hampel, W. *Int. Conf. Neutrino Physics & Astrophysics*, Hawaii, USA, July 1–8, 1981.
12. Burg, A.B.; Schlesinger, H.I. J. Am. Chem. Soc. **1937**, *59*, 780.
13. Schlesinger, H.I.; Brown, H.C.; Hoekstra, H.R.; Rapp, L.R. J. Am. Chem. Soc. **1953**, *75*, 199.
14. Schlesinger, H.I.; Brown, H.C.; Gilbreath, J.R.; Katz, J.J. J. Am. Chem. Soc. **1953**, *75*, 195.
15. Lane, C.F. Aldrichimica Acta **1973** *6*, 51.
16. Brown, H.C.; Krishnamurthy, S. Tetrahedron **1979**, *35*, 567.
17. Hutchins, R.O.; Learn, K.; Nazeir, B.; Pytlewski, D.; Petler, A. Org. Prep. Proc. Intl. **1984**, *16*, 335.
18. Jones, W.M. J. Am. Chem. Soc. **1960**, *82*, 2528.
19. Warshawsky, A.; Upson, D.A.; Ferrar, W.T.; Monnier, J.R. J. Polym. Sci. Part A Polym. Chem. **1989**, *27*, 3015.
20. Amelina, N.V.; Kalatskaya, L.V.; Gaevskaya, T.V. Vestsi Akad. Nauk BSSR, Ser. Khim. Navuk **1990**, *1*, 48. (in Russian)
21. Shelkovnikov, V.V.; Myakishev, K.G.; Kovalev, D.V.; Eroshkin, V.I.; Volkov, V.V. Zh. Nauchn. Prikl. Fotogr. Kinematogr. **1990**, *35*, 42. (in Russian)
22. Davis, R.E.; Brown, A.E.; Hopmann, R.; Kibby, C.L. J. Am. Chem. Soc. **1963**, *85*, 487.
23. Davis, R.E.; Bromels, E.; Kibby, C.L. J. Am. Chem. Soc. **1962**, *84*, 885.
24. Ryschkewitsch, G.E. J. Am. Chem. Soc. **1960**, *82*, 3290.
25. Davis, R.E. J. Am. Chem. Soc. **1962**, *84*, 892.
26. Brown, H.C.; Murray, L.T. Inorg. Chem. **1984**, *23*, 2746.
27. Hawthorne, M.F.; Miller, J.J. J. Am. Chem. Soc. **1958**, *80*, 754.
28. Shapiro, I.; Lustig, M.; Williams, R.E. J. Am. Chem. Soc. **1959**, *81*, 838.

29. Miller, J.J.; Hawthorne, M.F. J. Am. Chem. Soc. **1959**, *81*, 4501.
30. Palchak, R.F.; Horman, J.H.; Williams, R.E. J. Am. Chem. Soc. **1961**, *83*, 3380.
31. Kreevoy, M.M.; Hutchins, J.E.C. J. Am. Chem. Soc. **1969**, *91*, 4329.
32. Borch, F.R. J. Am. Chem. Soc. **1969**, *91*, 3996.
33. Schaeffer, G.F.; Anderson, E.R. J. Am. Chem. Soc. **1949**, *71*, 2143.
34. Kampel, V.; Warshawsky, A. J. Organomet. Chem. **1994**, *15*, 469.
35. Muraviev, D.; Rogachev, I.; Bromberg, L.; Warshawsky, A. J. Phys. Chem. **1994**, *98*, 718.
36. Carpenter, J.D.; Ault, B.S. J. Phys. Chem. **1991**, *95*, 3507.
37. Muraviev, D.; Warshawsky, A. React. & Funct. Polym. **1996**, *29*, 185.
38. Bromberg, L.; Muraviev, D.; Warshawsky, A. J. Phys. Chem. **1993**, *97*, 13927.
39. Starks, C.M. J. Am. Chem. Soc. **1971**, *93*, 195.
40. Spillane, W.J.; Don, H.J.-M.; Metzger, J. Tetrahedron Lett. **1976**, *26*, 2269.
41. Small, H. J. Am. Chem. Soc. **1968**, *90*, 2217.
42. Regen, S.L. J. Am. Chem. Soc. **1976**, *98*, 6270.
43. Regen, S.L. J. Org. Chem. **1977**, *42*, 875.
44. Helfferich, F. *Ion Exchange;* McGraw-Hill: New York, 1962.
45. Muraviev, D.; Warshawsky, A. React. Polym. **1994**, *22*, 55.
46. Drucker, C. Trans. Farad. Soc. **1937**, *33*, 60.
47. Högfeldt, E.; Bigeleisen, J. J. Am. Chem. Soc. **1960**, *82*, 15.
48. Laughton, P.M.; Robertson, R.E. In *Solute-Solvent Interactions*; Coetzee, J.F., Ritchie, C.D., Eds.; Marcel Dekker: New York, 1969; ch. 7, 399.
49. Dorfner, K. In *Ion Exchangers*; Dorfner, K., Ed.; Walter de Gruyter: Berlin, 1991; 82.
50. Muraviev, D.; Oleinikova, M.; Valiente, M. Langmuir **1997**, *13* (18), 4915.
51. Oleinikova, M.; Muraviev, D.; Valiente, M. Anal. Chem. **1999**, *71* (21), 4866.
52. Muraviev, D.; Torrado, A.; Valiente, M. *Extraction of Non-extractable Ionic Species in Aqua Impregnated Resin Systems*, presented at ISEC'99, Barcelona, Spain, July 11–16, 1999; Book of Abstracts, 122.
53. Cerrai, E. Chromatogr. Rev. **1964**, *6*, 129.
54. Braun, T.; Ghersini, G. *Extraction Chromatography;* Elsevier: New York, 1975.
55. Warshawsky, A. Talanta **1974**, *21*, 624.
56. Warshawsky, A. Trans. Inst. Min. Metall. **1974**, *83*, C101.
57. Warshawsky, A. In *Ion Exchange and Solvent Extraction;* Marinsky, J.A., Marcus, Y., Eds.; Marcel Dekker: New York, 1981; Vol. 8, chapter 3.
58. Muraviev, D. Chem. Scripta **1989**, *29*, 9.
59. Cortina, J.L.; Warshawsky, A. In *Ion Exchange and Solvent Extraction*; Marinsky, J.A., Marcus, Y., Eds.; Marcel Dekker: New York; 1997; Vol. 13, chapter 5.

60. Muraviev, D. Solv. Extr. Ion Exch. **1998**, *16* (1), 381.
61. Muraviev, D. Solv. Extr. Ion Exch. **2000**, *18* (4), 753.
62. Bromberg, L.; Muraviev, D.; Warshawsky, A. J. Phys. Chem. **1993**, *97*, 967.
63. Bromberg, L. J. Membr. Sci. **1991**, *62*, 131.

Marcel Dekker, Inc.
270 Madison Avenue, New York, New York 10016

Downloaded At: 10:46 25 January 2011

Request Permission or Order Reprints Instantly!

Interested in copying and sharing this article? In most cases, U.S. Copyright Law requires that you get permission from the article's rightsholder before using copyrighted content.

All information and materials found in this article, including but not limited to text, trademarks, patents, logos, graphics and images (the "Materials"), are the copyrighted works and other forms of intellectual property of Marcel Dekker, Inc., or its licensors. All rights not expressly granted are reserved.

Get permission to lawfully reproduce and distribute the Materials or order reprints quickly and painlessly. Simply click on the "Request Permission/Reprints Here" link below and follow the instructions. Visit the U.S. Copyright Office for information on Fair Use limitations of U.S. copyright law. Please refer to The Association of American Publishers' (AAP) website for guidelines on Fair Use in the Classroom.

The Materials are for your personal use only and cannot be reformatted, reposted, resold or distributed by electronic means or otherwise without permission from Marcel Dekker, Inc. Marcel Dekker, Inc. grants you the limited right to display the Materials only on your personal computer or personal wireless device, and to copy and download single copies of such Materials provided that any copyright, trademark or other notice appearing on such Materials is also retained by, displayed, copied or downloaded as part of the Materials and is not removed or obscured, and provided you do not edit, modify, alter or enhance the Materials. Please refer to our Website User Agreement for more details.

Order now!

Reprints of this article can also be ordered at

http://www.dekker.com/servlet/product/DOI/101081SS100104767